AGU PUBLICATIONS

Geophysical Research Letters

RESEARCH LETTER
10.1002/2014GL060111

Key Points:
- Ice losses from West Antarctica are 31% higher than last reported in IMBIE
- Snowfall gains and ice dynamical losses in East Antarctica have both diminished
- CryoSat surveys 96% of Antarctica with 5 times better sampling of coastal region

Supporting Information:
- Readme
- Figure S1
- Text S1

Correspondence to:
A. Shepherd,
a.shepherd@leeds.ac.uk

Citation:
McMillan, M., A. Shepherd, A. Sundal, K. Briggs, A. Muir, A. Ridout, A. Hogg, and D. Wingham (2014), Increased ice losses from Antarctica detected by CryoSat-2, *Geophys. Res. Lett.*, *41*, 3899–3905, doi:10.1002/2014GL060111.

Received 3 APR 2014
Accepted 15 MAY 2014
Accepted article online 16 MAY 2014
Published online 9 JUN 2014

Increased ice losses from Antarctica detected by CryoSat-2

Malcolm McMillan[1], Andrew Shepherd[1,2], Aud Sundal[1], Kate Briggs[1], Alan Muir[2], Andrew Ridout[2], Anna Hogg[1], and Duncan Wingham[2]

[1]Centre for Polar Observation and Modelling, School of Earth and Environment, University of Leeds, Leeds, UK, [2]Centre for Polar Observation and Modelling, Department of Earth Sciences, University College London, London, UK

Abstract We use 3 years of Cryosat-2 radar altimeter data to develop the first comprehensive assessment of Antarctic ice sheet elevation change. This new data set provides near-continuous (96%) coverage of the entire continent, extending to within 215 km of the South Pole and leading to a fivefold increase in the sampling of coastal regions where the vast majority of all ice losses occur. Between 2010 and 2013, West Antarctica, East Antarctica, and the Antarctic Peninsula changed in mass by -134 ± 27, -3 ± 36, and -23 ± 18 Gt yr^{-1}, respectively. In West Antarctica, signals of imbalance are present in areas that were poorly surveyed by past missions, contributing additional losses that bring altimeter observations closer to estimates based on other geodetic techniques. However, the average rate of ice thinning in West Antarctica has also continued to rise, and mass losses from this sector are now 31% greater than over the period 2005–2010.

1. Introduction

With a capacity to resolve detailed patterns of elevation change at the scale of glacier drainage basins [*Shepherd et al*., 2002; *Davis and Ferguson*, 2004; *Pritchard et al*., 2009; *Remy and Parouty*, 2009; *Shepherd et al*., 2004; *Wingham et al*., 2006; *Zwally et al*., 2005], repeat satellite altimetry has transformed our ability to study the polar ice sheets. Nevertheless, direct measurements of elevation change have been restricted by the latitudinal limits of satellite altimeter orbits (81.5° and 86.0° for conventional radar and laser systems, respectively), by the reduced performance of conventional radar altimeters over the steep terrain that is typical of ice sheet margins and by the irregular temporal sampling of satellite laser altimeter data due to the episodic nature of ICESat mission campaigns and due to the presence of clouds. These limitations have precluded, for example, comprehensive assessments of Antarctic Peninsula volume change, and altimeter data omission may also explain differences in mass balance estimates for other ice sheet regions [*Shepherd et al*., 2012]. CryoSat-2 was designed to overcome several of the limiting factors that previous satellite altimeters faced, with an orbital limit extending to 88° and a novel synthetic aperture radar interferometry mode providing measurements of fine spatial resolution in areas of steep terrain [*Wingham et al*., 2006]. Here we use CryoSat-2 data acquired between November 2010 and September 2013 to produce the first altimeter-derived estimates of volume and mass change for the entire Antarctic ice sheet.

2. Data and Methods

To compute changes in ice sheet elevation, we adapted a repeat-track method [*Flament and Remy*, 2012; *Moholdt et al*., 2010; *Smith et al*., 2009] to suit the Cryosat-2 data set, which provides high and low spatial and temporal sampling, respectively, relative to other altimeter missions (see supporting information). Altogether, Cryosat-2 has acquired 159 million range measurements across inland and coastal sectors of Antarctica in pulse-limited and synthetic aperture radar interferometry modes, and we process measurements from each mode in an identical manner. Ice sheet elevation is calculated as the difference between satellite locations and range measurements corrected for the lag of the leading edge tracker [*Wingham et al*., 2006], fluctuations in dry and wet atmospheric mass, the effects of the ionosphere, isostatic rebound [*Ivins et al*., 2013; *Whitehouse et al*., 2012], and for solid Earth and ocean tides. Elevation measurements are accumulated in 469,451 regularly spaced (5 by 5 km) geographical regions, and within each region, we solve, simultaneously, for spatial and temporal fluctuations in elevation and for a fixed contribution due to the impact of surface anisotropy on the tracked range (see supporting information). As part of this calculation, outlying data are

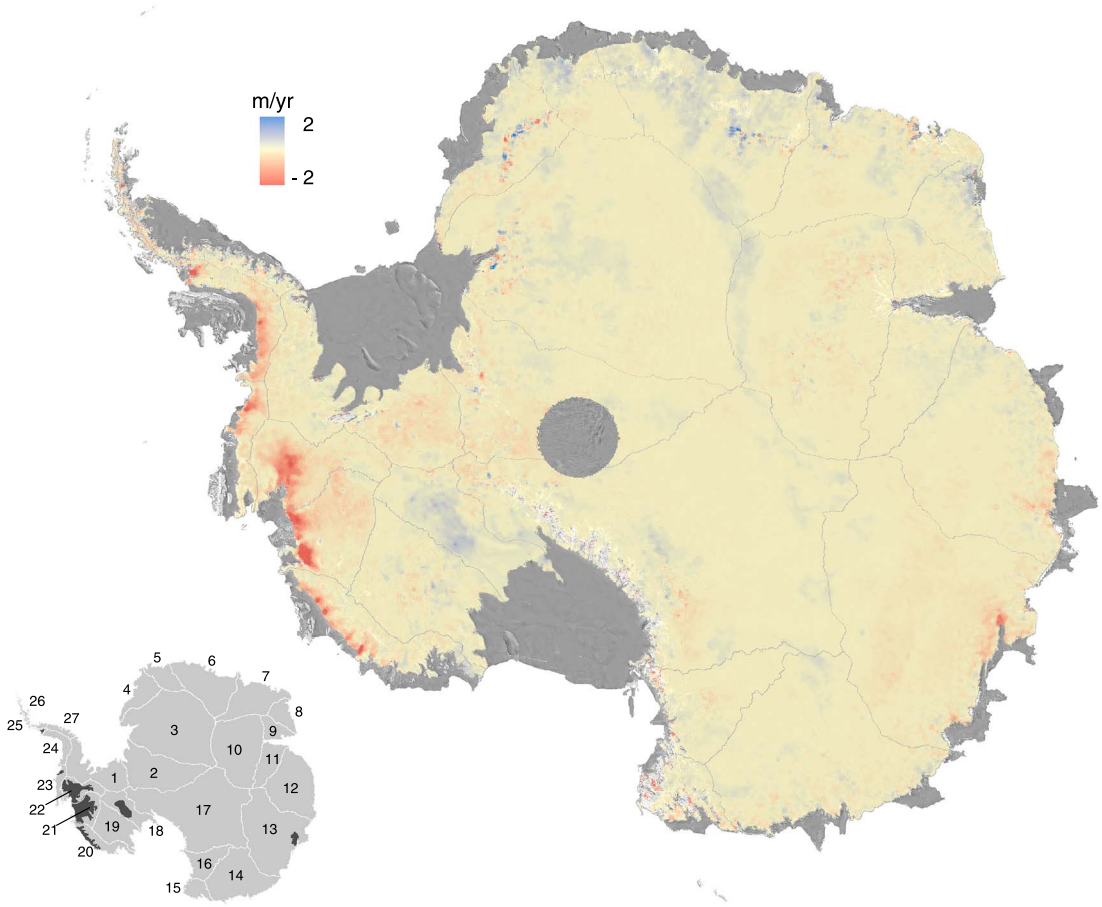

Figure 1. Rate of elevation change of the Antarctic ice sheet between 2010 and 2013 determined from CryoSat-2 repeat altimetry and smoothed with a 25 by 25 km median filter. Solid grey and white (inset) lines show the boundaries of 27 ice sheet drainage basins [*Zwally et al.*, 2012]. The CryoSat measurements reach to within 215 km of the South Pole, as compared to 930 and 430 km for the ERS/Envisat and ICESat altimeters, respectively. Also shown (inset) are the numbers used to identify ice sheet drainage basins, with East Antarctica and the Antarctic Peninsula defined as basins 2 to 17 and 24 to 27, respectively, and West Antarctica defined as the remaining basins and the mask developed (see supporting information) to identify elevation changes occurring at the density of ice (inset, black regions). Elsewhere, we assume that elevation changes are caused by fluctuations in surface mass balance alone, and we therefore applied a density of snow to these signals (inset, grey regions). Ice dynamical imbalance (IDI) is evident as thickening of the Kamb Ice Stream (basin 18) and as widespread thinning across the Amundsen Sea sector (basins 21 and 22), with the latter signal affecting a considerably larger area than at any time in the past two decades [*Shepherd et al.*, 2002, 2004; *Wingham et al.*, 2009].

culled, iteratively, to minimize their impact on each solution, and a correction is then applied to account for temporal fluctuations in backscatter that cause spurious fluctuations in range [*Davis and Ferguson*, 2004; *Khvorostovsky*, 2012; *Wingham et al.*, 1998]. After editing the resulting trends to remove 14,098 poorly constrained solutions, we obtain 455,403 independent estimates of elevation change distributed across 96% of the grounded Antarctic ice sheet (Figure 1), with an effective average temporal resolution of 60 days. We compute the uncertainty of area-averaged elevation trends from the root-sum-square of the uncertainties determined from contributing model fits (see supporting information), as errors associated with altimeter elevation measurements have been shown to rapidly decorrelate with increasing spatial separation [*Wingham et al.*, 1998].

We assessed the degree to which the CryoSat-2 orbit pattern and interferometric mode of operation provide improved detection of ice sheet elevation changes relative to past altimeters. The data (Figure 1) show several geographically isolated regions of surface uplift and lowering interspersed with wide areas of no overall change, and, altogether, their extent is a significant improvement on that afforded by earlier missions [*Pritchard et al.*, 2009; *Wingham et al.*, 1998]. For example, the region of unsurveyed ice at the South Pole is now only 147,725 km^2 in area −1.2% of the grounded ice sheet and 18 and 4 times smaller

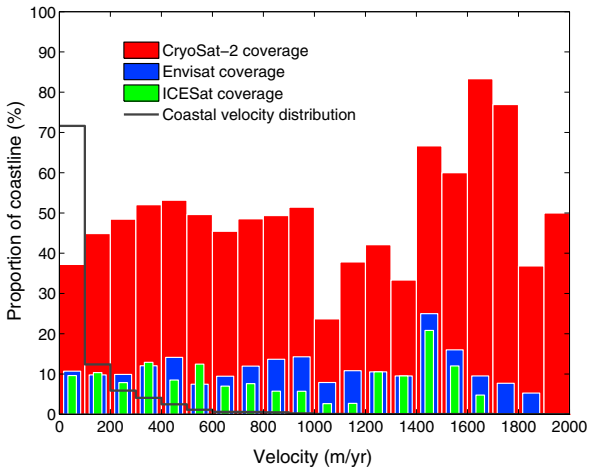

Figure 2. Distribution of ice velocity [*Rignot et al.*, 2011b] at 55,440 regularly spaced locations around the margin of the Antarctic ice sheet (black) and the proportion of these locations surveyed on six or more occasions by the Envisat (blue), ICESat (green), and CryoSat (red) altimeters. The ice sheet margin was mapped from a digital database [*British Antarctic Survey*, *Scott Polar Research Institute*, *and World Conservation Monitoring Centre*, 1993] augmented with interferometric synthetic aperture radar observations [*Rignot et al.*, 2011a], and ice velocities were extracted where this boundary intersected a 900 m resolution gridded map of ice speed derived from synthetic aperture radar measurements [*Rignot et al.*, 2011b]. Although only a small fraction (2.5%) of the ice sheet margin flows at speeds in excess of 500 m/yr, these fast-moving ice streams and outlet glaciers channel the majority of ice into the ocean and include the principal locations of contemporary dynamical imbalance [*Shepherd and Wingham*, 2007]. The Envisat, ICESat, and CryoSat altimeters have surveyed 10, 8, and 49% of the coastal region with sufficient frequency to detect temporal changes in elevation, respectively.

than that of the Envisat and ICESat missions, respectively. In addition, the rugged terrain of the continental margin —where the vast majority of known imbalance has occurred—is now densely surveyed, including the majority of the mountainous Antarctic Peninsula and the grounding zones of Totten Glacier (116°E) and of Marie Byrd Land (103° to 158°W). Altogether, CryoSat-2 has surveyed 49% of the Antarctic coastal region on six or more occasions, 6 and 5 times more than the Envisat (8%) and ICESat (10%) altimeters, respectively (Figure 2). Moreover, CryoSat-2 has surveyed 62% of the fastest-flowing ice ($>1500\,\mathrm{m\,yr^{-1}}$) where dynamic thinning is concentrated ~10 times more than other missions. Although there is no obvious difference between the interferometric mode elevation rates and those determined in the traditional pulse-limited altimeter mode (Figure 1), we nevertheless compared them to ~25,000 independent estimates derived from coincident repeat airborne laser altimetry (see supporting information) to assess their certainty. In the Amundsen Sea sector of West Antarctica where rates of ice thickness change are varied and large, elevation rates determined from ~85,000 CryoSat-2 measurements are in close agreement with these airborne observations (Figure 3); after adjusting for bias introduced by the airborne sampling pattern (see supporting information), the root-mean-square difference ($34\,\mathrm{cm\,yr^{-1}}$) is smaller than the expected elevation fluctuation due to snowfall variability.

3. Results

The CryoSat-2 observations confirm the continuation of existing signals of elevation change [*Pritchard et al.*, 2009; *Shepherd et al.*, 2002, 2012; *Wingham et al.*, 1998; *Zwally et al.*, 2005], identify regions which have evolved since previous surveys, and allow investigations of new terrain. Between 2010 and 2013, the average elevation of the Antarctic ice sheet fell by $1.9 \pm 0.2\,\mathrm{cm\,yr^{-1}}$. Although most of the observed changes are smaller than expected fluctuations in snowfall (Table 1), those that are not coincide with areas of known dynamical imbalance (basins 13, 18, and 20 to 22) or with episodes of anomalous snow accumulation (basin 6) [*Lenaerts et al.*, 2013]. Overall, the pattern of elevation change is still dominated by widespread glacier thinning across the Amundsen and Bellingshausen Sea sectors (basins 20–24), with maximum rates of surface lowering reaching $9\,\mathrm{m\,yr^{-1}}$ at Smith Glacier. Ice catchments feeding this 3500 km stretch of coastline are now thinning at an average rate of $30 \pm 0.5\,\mathrm{cm\,yr^{-1}}$. In the Ross Sea sector (basin 18), ice stream deceleration [*Joughin et al.*, 2002] continues to drive widespread thickening of the Kamb Ice Stream and of faster flowing sections of the Whillans Ice Stream, at rates in excess of $50\,\mathrm{cm\,yr^{-1}}$. In East Antarctica, although there are mesoscale patterns of modest surface uplift (e.g., basin 6) and lowering (e.g., basin 13) that are typical of snowfall variability [*Davis et al.*, 2005; *Monaghan et al.*, 2006; *Lenaerts et al.*, 2013], there is no significant change in elevation, overall, across the slow-flowing interior (Figure 1). However, with detailed sampling of coastal regions, our data set does reveal,

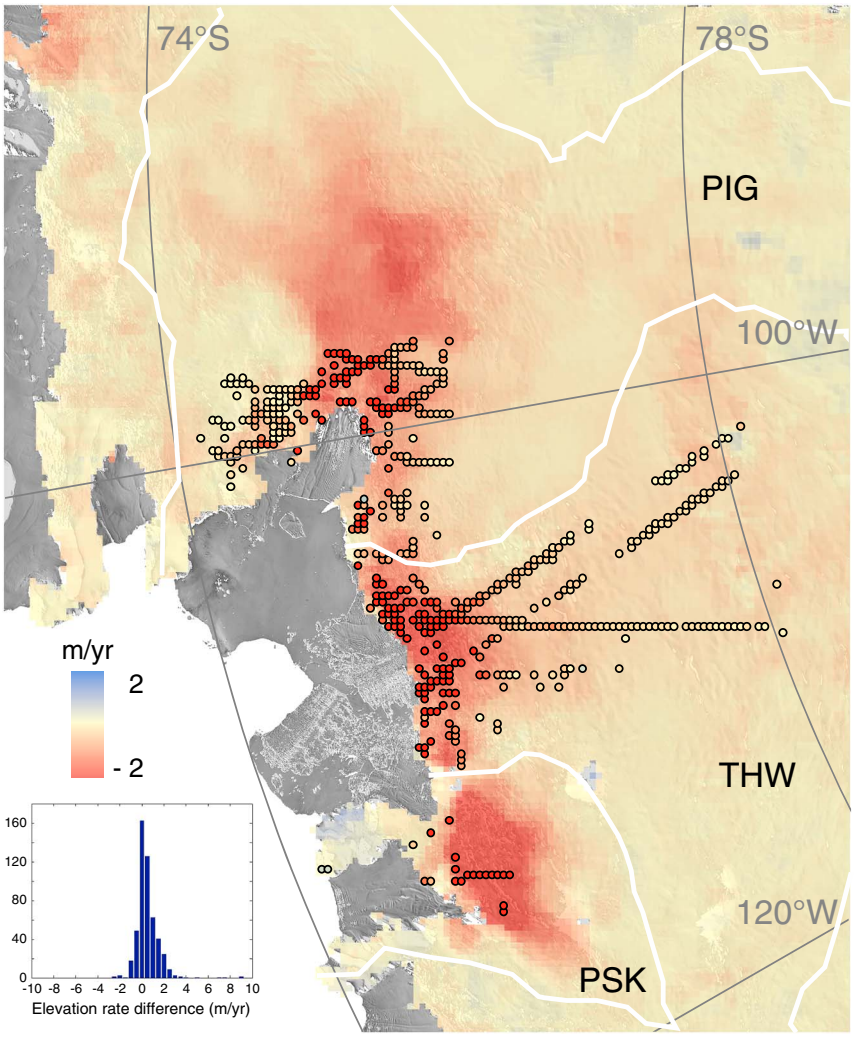

Figure 3. Surface elevation change of the Amundsen Sea sector, West Antarctica, determined from CryoSat-2 (2010 to 2013) and, overlaid, from repeat airborne laser altimetry gridded at 5 km spacing (2009 to 2012) (see supporting information). White boundaries delineate the drainage basins of the Pine Island Glacier (PIG), the Thwaites Glacier (THW), and the Pope/Smith/Kohler glaciers (PSK). (inset) Distribution of the difference (CryoSat minus airborne) between 495 coincident CryoSat and airborne elevation rates, after accounting for a 15% bias introduced by the irregular sampling pattern of the airborne measurements (see supporting information). The root-mean-square difference in elevation rate determined using the CryoSat and airborne measurements is 54 cm yr^{-1}; 21 cm yr^{-1} of which can be explained by the airborne sampling bias, and the remainder can be explained by either a fluctuation in snow accumulation due to the 1 year mismatch in observation period (38 cm yr^{-1}, based on the data in Table 1) or the uncertainties of the airborne and satellite measurements themselves (17 and 16 cm yr^{-1}, respectively).

for the first time, that thinning of the Totten Glacier (basin 13) extends to its grounding line [*Rignot et al.*, 2011a] and is everywhere correlated with fast ice flow. In contrast, the Cook glacier (basin 14), which thinned at modest rates during previous surveys [*Shepherd et al.*, 2012], shows no significant change in elevation since 2010.

We calculated rates of mass change within all Antarctic drainage basins [*Zwally et al.*, 2012] using a surface-density model (see Figure 1, inset) to discriminate between elevation fluctuations occurring at the densities of snow and ice. To delimit these regions, we updated an earlier classification scheme [*Shepherd et al.*, 2012] to include additional information on ice flow (see supporting information). In calculating the mass imbalance, we treat both the elevation rate error and snowfall variability as sources of uncertainty (see supporting information). Between 2010 and 2013, we estimate that West Antarctica, East Antarctica, and the Antarctic Peninsula changed in mass by -134 ± 27, -3 ± 36, and -23 ± 18 Gt yr^{-1},

Table 1. The Area, Mean Accumulation Rate, Estimated Snowfall Variability, Average Elevation Rate, and Estimated Mass Imbalance of Antarctic Drainage Basins (Numbered 1–27) and of Regions of Ice Dynamical Imbalance (IDI) (see Figure 1) From 2010 to 2013[a]

Basin	Observed Area[b] (km^2)	Mean Ice Accumulation Rate[c] (cm/yr)	Snowfall Variability[d] (cm/yr)	Mean Elevation Rate (cm/yr)	Mass Imbalance (Gt/yr)
1	443,250	29.1	8.4	−4.9 ± 0.2	−8 ± 14
2	584,550	9.1	2.1	−1.4 ± 0.1	−4 ± 6
3	1,493,425	6.4	1.1	1.1 ± 0.1	6 ± 6
4	226,625	20.0	7.8	1.5 ± 0.5	1 ± 7
5	177,100	16.6	7.7	6.5 ± 0.5	4 ± 5
6	583,050	12.6	3.5	13.5 ± 0.2	28 ± 8
7	481,275	15.1	4.6	2.3 ± 0.2	4 ± 8
8	157,525	18.0	8.8	8.3 ± 0.4	5 ± 5
9	139,175	13.5	7.8	−0.3 ± 0.5	0 ± 4
10	886,950	5.9	1.2	−0.8 ± 0.1	−3 ± 4
11	248,275	7.1	2.8	0.8 ± 0.2	1 ± 3
12	714,475	22.9	6.3	−2.1 ± 0.1	−5 ± 16
13	1,101,250	22.0	5.0	−8.4 ± 0.1	−39 ± 20
Totten IDI	*20,225*	*69.7*	*36.6*	*−52.2 ± 1.2*	*−10 ± 3*
14	702,400	20.7	5.1	0.4 ± 0.1	1 ± 13
15	81,350	18.4	10.0	−5.7 ± 1.7	−2 ± 5
16	238,750	11.2	4.5	−1.9 ± 0.4	−2 ± 4
17	1,683,725	7.6	1.2	0.3 ± 0.1	2 ± 8
18	253,500	14.0	5.2	17.4 ± 0.2	29 ± 5
Kamb IDI	*51,150*	*12.9*	*6.7*	*46.2 ± 0.4*	*22 ± 1*
19	355,900	14.5	4.5	0.7 ± 0.2	1 ± 6
20	168,700	30.7	13.7	−15.9 ± 0.5	−23 ± 9
Getz IDI	*33,200*	*37.5*	*19.4*	*−70.4 ± 1.1*	*−22 ± 3*
21	205,650	37.2	15.1	−36.2 ± 0.4	−64 ± 12
Thwaites IDI	*91,850*	*44.5*	*22.8*	*−37.5 ± 0.5*	*−32 ± 8*
PSK IDI	*20,950*	*37.9*	*19.6*	*−117.5 ± 1.3*	*−25 ± 2*
22	207,325	42.9	17.5	−32.7 ± 0.3	−56 ± 13
Pine Island IDI	*96,800*	*47.7*	*24.5*	*−59.4 ± 0.4*	*−53 ± 9*
23	70,850	67.8	35.2	−30.6 ± 0.8	−12 ± 9
Ferrigno IDI	*5,950*	*74.4*	*38.2*	*−123.7 ± 2.7*	*−7 ± 1*
24	92,700	57.7	30.3	−32.2 ± 0.8	−11 ± 11
25	17,600	110.8	63.4	−52.3 ± 4.8	−9 ± 9
26	21,925	103.2	61.1	−24.6 ± 4.2	−4 ± 9
27	35,100	55.5	29.9	4.8 ± 2.9	1 ± 6
East Antarctica	**9,499,900**	**11.6**	**1.0**	**0.1 ± 0.2**	**−3 ± 36**
West Antarctica	**1,705,175**	**26.0**	**4.4**	**−9.8 ± 0.3**	**−134 ± 27**
Antarctic Peninsula	**167,325**	**67.6**	**32.4**	**−25.6 ± 2.5**	**−23 ± 18**
Antarctica	**11,372,400**	**14.8**	**1.2**	**−1.9 ± 0.2**	**−159 ± 48**

[a]Few regions exhibit elevation fluctuations that are large in comparison to expected snowfall variability over the 3 year survey. The boldface signifies subtotal (East Antarctica, West Antarctica, and Antarctic Peninsula) and total (Antarctica) values.
[b]Derived from the map of *Zwally et al.* [2012].
[c]Derived from *Vaughan et al.* [1999] and assuming an ice density of 917 kg m^{-3}.
[d]Following the method of *Wingham et al.* [1998] and assuming a snow density of 350 kg m^{-3}.

respectively (Table 1). The largest signal of imbalance occurred in the Amundsen Sea sector (basins 21 and 22) which lost a total of 120 ± 18 Gt yr^{-1} over the course of our study period −90% of the entire West Antarctic mass loss. The Cryosat-2 data set also reveals greater rates of mass loss from the main outlet glaciers of the Amundsen Sea sector, compared to observations acquired by ERS and Envisat between 1992 and 2010 [*Shepherd et al*., 2012] (Figure 4). While these differences are due to increases in the average rate of ice thinning, changes elsewhere—particularly in areas of steep coastal terrain—are in part due to the improved sampling of Cryosat-2. For example, CryoSat-2 now surveys 97% of glaciers flowing into the Getz Ice Shelf (basin 20), significantly more than either ERS (36%) or Envisat (72%), and the net effect is a threefold increase in the estimated volume change within the basin compared to a twofold increase in the coincident rate of thinning.

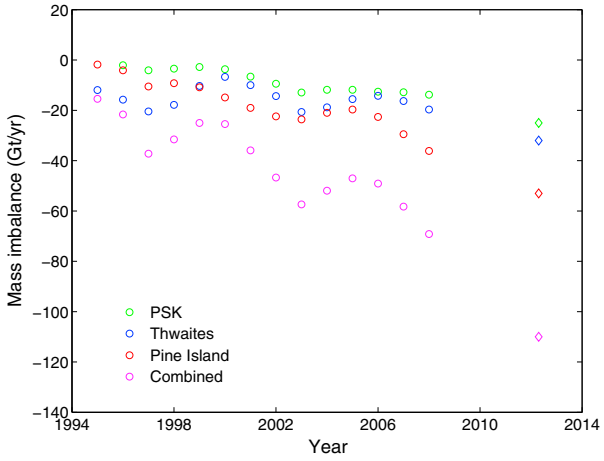

Figure 4. Rate of mass change of areas of unbalanced ice flow (see Figure 1) within the Pine Island (red), Thwaites (blue), and Pope/Smith/Kohler (PSK) (green) glacier drainage basins (Figure 3), as well as the total area of dynamical imbalance within the Amundsen Sea sector (magenta). Trends are calculated over 6 year periods between 1992 and 2010 using a 19 year time series of ERS-1, ERS-2, and Envisat data (circles) and over a 3 year period using CryoSat-2 data acquired between 2010 and 2013 (diamonds).

4. Discussion

Our measurements of Antarctic ice sheet volume change extend the record of ice sheet mass balance to the present day. In the Amundsen Sea sector, where ice losses have tripled over the past two decades [*Medley et al.*, 2014; *Rignot et al.*, 2008; *Wingham et al.*, 2009], our estimates of imbalance are in close agreement with those determined using independent methods. For example, according to mass budget estimates, the Pine Island Glacier —which remains the largest individual source of global ocean mass—lost 44 ± 7 Gt of ice in the year 2011 [*Medley et al.*, 2014], a value that is consistent with our estimate (56 ± 13 Gt yr^{-1}) derived over the period 2010 to 2013 and over an 11% larger area. Similarly, our estimate of the specific rate of mass loss from the wider, 419,000 km^2 Amundsen Sea sector (286 ± 42 kg m^{-2} yr^{-1}) is comparable to that derived for 89% of the same area using the mass budget approach (260 ± 35 kg m^{-2} yr^{-1} in *Medley et al.* [2014]). Although ice discharge from the Pine Island Glacier has remained stable since 2010 [*Medley et al.*, 2014] following a notable decrease in the rate of ocean melting at the glacier terminus [*Dutrieux et al.*, 2014], the period of the CryoSat-2 measurements is too short to establish whether the inland progression of ice thinning has abated.

At the continental scale, the most recent estimates of Antarctic ice sheet mass balance are based solely on satellite gravimetry surveys [*Barletta and Bordoni*, 2013; *Velicogna and Wahr*, 2013; *Williams et al.*, 2014]. According to these studies, the rate of ice mass loss from Antarctica has increased progressively over the past decade and, between 2010 and 2012, fell in the approximate central range 105 to 130 Gt yr^{-1}. Our survey puts the contemporary rate of Antarctic ice sheet mass loss at 159 ± 48 Gt yr^{-1}, a value that, although larger, is nevertheless consistent given the spread of the gravimetry-based uncertainties (16 to 80 Gt yr^{-1}). A possible explanation for the discrepancy is the exceptional snowfall event of 2009, which saw an additional ~200 Gt of mass deposited in East Antarctica [*Boening et al.*, 2012; *Lenaerts et al.*, 2013; *Shepherd et al.*, 2012] that, although absent from the CryoSat-2 record, does factor in the gravimetry-based estimates of imbalance. It is also worth noting that gravimetry-based estimates of Antarctic ice sheet mass balance remain sensitive to the choice of model used to correct for glacial isostatic adjustment, with differences of up to 64 Gt yr^{-1} arising when alternative models are employed [*Velicogna and Wahr*, 2013], reinforcing the need for contemporaneous estimates of ice mass loss derived from independent techniques [*Shepherd et al.*, 2012].

5. Conclusions

We estimate that, since 2010, the average Antarctic ice sheet contribution to global sea level rise has been 0.45 ± 0.14 mm yr^{-1}. This value, which is more than twice as large as the 20 year mean determined from an ensemble of geodetic techniques (0.19 ± 0.15 mm yr^{-1} in *Shepherd et al.* [2012]), reflects both the improved capability of CryoSat-2 to observe regions of ice dynamical imbalance and the impact of short- and intermediate-term changes in ice sheet mass. In West Antarctica, there is now little doubt that the rate of ice loss has continued to rise and that with over 97% sampling of this region, this increase is now well resolved. However, in East Antarctica and at the Antarctic Peninsula, the average change in ice sheet mass remains small in comparison to expected fluctuations in snow accumulation (Table 1), which present an observational challenge to all geodetic techniques. Although the CryoSat-2 measurements allow an improved understanding of the drivers and timescales of ice sheet imbalance in these sectors, longer-period data sets are required to separate the effects of meteorological and ice dynamical imbalance [*Wouters et al.*, 2013].

Nevertheless, the fine spatial and temporal resolution of ice sheet elevation changes afforded by interferometric synthetic aperture radar altimetry represents a remarkable advance on the capability of past missions and provides greater confidence in assessments of ice sheet mass imbalance.

Acknowledgments
This work was supported by the UK Natural Environment Research Council. The CryoSat-2 and airborne altimetry data used in this study are available from the European Space Agency and the National Snow and Ice Data Center, respectively. We are grateful to the Editor and to two reviewers for their comments, which helped improve the manuscript.

The Editor thanks two anonymous reviewers for their assistance in evaluating this paper.

References

Barletta, V. R., and A. Bordoni (2013), Effect of different implementations of the same ice history in GIA modeling, *J. Geodyn.*, *71*, 65–73, doi:10.1016/j.jog.2013.07.002.

Boening, C., M. Lebsock, F. Landerer, and G. Stephens (2012), Snowfall-driven mass change on the East Antarctic ice sheet, *Geophys. Res. Lett.*, *39*, L21501, doi:10.1029/2012GL053316.

British Antarctic Survey, Scott Polar Research Institute, and World Conservation Monitoring Centre (1993), Antarctic digital database.

Davis, C. H., and A. C. Ferguson (2004), Elevation change of the Antarctic ice sheet, 1995–2000, from ERS-2 satellite radar altimetry, *IEEE Trans. Geosci. Remote Sens.*, *42*(11), 2437–2445, doi:10.1109/TGRS.2004.836789.

Davis, C. H., Y. H. Li, J. R. McConnell, M. M. Frey, and E. Hanna (2005), Snowfall-driven growth in East Antarctic ice sheet mitigates recent sea-level rise, *Science*, *308*(5730), 1898–1901, doi:10.1126/science.1110662.

Dutrieux, P., J. De Rydt, A. Jenkins, P. R. Holland, H. K. Ha, S. H. Lee, E. J. Steig, Q. H. Ding, E. P. Abrahamsen, and M. Schroder (2014), Strong sensitivity of pine island ice-shelf melting to climatic variability, *Science*, *343*(6167), 174–178, doi:10.1126/science.1244341.

Flament, T., and F. Remy (2012), Dynamic thinning of Antarctic glaciers from along-track repeat radar altimetry, *J. Glaciol.*, *58*(211), 830–840, doi:10.3189/2012JoG11J118.

Ivins, E. R., T. S. James, J. Wahr, E. J. Schrama, F. W. Landerer, and K. M. Simon (2013), Antarctic contribution to sea level rise observed by GRACE with improved GIA correction, *J. Geophys. Res. Solid Earth*, *118*, 3126–3141, doi:10.1002/jgrb.50208.

Joughin, I., S. Tulaczyk, R. Bindschadler, and S. F. Price (2002), Changes in West Antarctic ice stream velocities: Observation and analysis, *J. Geophys. Res.*, *107*(B11), 2289, doi:10.1029/2001JB001029.

Khvorostovsky, K. S. (2012), Merging and analysis of elevation time series over Greenland Ice Sheet from satellite radar altimetry, *IEEE Trans. Geosci. Remote Sens.*, *50*(1), 23–36, doi:10.1109/TGRS.2011.2160071.

Lenaerts, J. T. M., E. van Meijgaard, M. R. van den Broeke, S. R. M. Ligtenberg, M. Horwath, and E. Isaksson (2013), Recent snowfall anomalies in Dronning Maud Land, East Antarctica, in a historical and future climate perspective, *Geophys. Res. Lett.*, *40*, 2684–2688, doi:10.1016/j.rse.2010.06.008.

Medley, B., et al. (2014), Constraining the recent mass balance of Pine Island and Thwaites glaciers, West Antarctica with airborne observations of snow accumulation, *Cryosphere Discuss.*, *8*(1), 953–998, doi:10.5194/tcd-8-953-2014.

Moholdt, G., C. Nuth, J. O. Hagen, and J. Kohler (2010), Recent elevation changes of Svalbard glaciers derived from ICESat laser altimetry, *Remote Sens. Environ.*, *114*(11), 2756–2767, doi:10.1016/j.rse.2010.06.008.

Monaghan, A. J., et al. (2006), Insignificant change in Antarctic snowfall since the International Geophysical Year, *Science*, *313*(5788), 827–831, doi:10.1126/science.1128243.

Pritchard, H. D., R. J. Arthern, D. G. Vaughan, and L. A. Edwards (2009), Extensive dynamic thinning on the margins of the Greenland and Antarctic ice sheets, *Nature*, *461*(7266), 971–975, doi:10.1038/nature08471.

Remy, F., and S. Parouty (2009), Antarctic ice sheet and radar altimetry: A review, *Remote Sens.*, *1*(4), 1212–1239, doi:10.3390/rs1041212.

Rignot, E., J. L. Bamber, M. R. van den Broeke, C. Davis, Y. H. Li, W. J. Van De Berg, and E. van Meijgaard (2008), Recent Antarctic ice mass loss from radar interferometry and regional climate modelling, *Nat. Geosci.*, *1*(2), 106–110, doi:10.1038/ngeo102.

Rignot, E., J. Mouginot, and B. Scheuchl (2011a), Antarctic grounding line mapping from differential satellite radar interferometry, *Geophys. Res. Lett.*, *38*, L10504, doi:10.1029/2011GL047109.

Rignot, E., J. Mouginot, and B. Scheuchl (2011b), Ice flow of the Antarctic ice sheet, *Science*, *333*(6048), 1427–1430, doi:10.1126/science.1208336.

Shepherd, A., and D. Wingham (2007), Recent sea-level contributions of the Antarctic and Greenland ice sheets, *Science*, *315*(5818), 1529–1532, doi:10.1126/science.1136776.

Shepherd, A., D. J. Wingham, and J. A. D. Mansley (2002), Inland thinning of the Amundsen Sea sector, West Antarctica, *Geophys. Res. Lett.*, *29*(10), 1364, doi:10.1029/2001GL014183.

Shepherd, A., D. Wingham, and E. Rignot (2004), Warm ocean is eroding West Antarctic Ice Sheet, *Geophys. Res. Lett.*, *31*, L23402, doi:10.1029/2004GL021106.

Shepherd, A., et al. (2012), A reconciled estimate of ice-sheet mass balance, *Science*, *338*(6111), 1183–1189, doi:10.1126/science.1228102.

Smith, B. E., H. A. Fricker, I. R. Joughin, and S. Tulaczyk (2009), An inventory of active subglacial lakes in Antarctica detected by ICESat (2003-2008), *J. Glaciol.*, *55*(192), 573–595, doi:10.3189/002214309789470879.

Vaughan, D. G., J. L. Bamber, M. Giovinetto, J. Russell, and A. P. R. Cooper (1999), Reassessment of net surface mass balance in Antarctica, *J. Clim.*, *12*(4), 933–946, doi:10.1175/1520-0442(1999)0122.0.CO;2.

Velicogna, I., and J. Wahr (2013), Time-variable gravity observations of ice sheet mass balance: Precision and limitations of the GRACE satellite data, *Geophys. Res. Lett.*, *40*, 3055–3063, doi:10.1002/grl.50527.

Whitehouse, P. L., M. J. Bentley, G. A. Milne, M. A. King, and I. D. Thomas (2012), A new glacial isostatic adjustment model for Antarctica: Calibrated and tested using observations of relative sea-level change and present-day uplift rates, *Geophys. J. Int.*, *190*(3), 1464–1482, doi:10.1111/j.1365-246X.2012.05557.x.

Williams, S. D. P., P. Moore, M. A. King, and P. L. Whitehouse (2014), Revisiting GRACE Antarctic ice mass trends and accelerations considering autocorrelation, *Earth Planet. Sci. Lett.*, *385*, 12–21, doi:10.1016/j.espl.2013.10.016.

Wingham, D. J., A. J. Ridout, R. Scharroo, R. J. Arthern, and C. K. Shum (1998), Antarctic elevation change from 1992 to 1996, *Science*, *282*(5388), 456–458, doi:10.1126/science.282.5388.456.

Wingham, D., et al. (2006), CryoSat: A mission to determine the fluctuations in Earth's land and marine ice fields, *Adv. Space Res.*, *37*(4), 841–871, doi:10.1016/j.asr.2005.07.027.

Wingham, D. J., D. W. Wallis, and A. Shepherd (2009), Spatial and temporal evolution of Pine Island Glacier thinning, 1995–2006, *Geophys. Res. Lett.*, *36*, L17501, doi:10.1029/2009GL039126.

Wouters, B., J. Bamber, M. van den Broeke, J. Lenaerts, and I. Sasgen (2013), Limits in detecting acceleration of ice sheet mass loss due to climate variability, *Nat. Geosci.*, *6*(8), 613–616, doi:10.1038/ngeo1874.

Zwally, H., M. B. Giovinetto, J. Li, H. G. Cornejo, M. A. Beckley, A. C. Brenner, J. L. Saba, and D. Yi (2005), Mass changes of the Greenland and Antarctic ice sheets and shelves and contributions to sea-level rise: 1992–2002, *J. Glaciol.*, *51*(175), 509–527, doi:10.3189/172756505781829007.

Zwally, H. J., M. B. Giovinetto, M. A. Beckley, and J. L. Saba (2012), Antarctic and Greenland drainage systems, GSFC Cryospheric Sciences Laboratory.